Observation of Nuclear Wave-Packet Interference in Ultrafast Interatomic Energy Transfer

Meng Han[1], Jacqueline Fedyk,[2] Jia-Bao Ji,[1] Victor Despré,[2,3]
Alexander I. Kuleff[2,*] and Hans Jakob Wörner[1,†]

[1]*Laboratorium für Physikalische Chemie, ETH Zürich, 8093 Zürich, Switzerland*
[2]*Theoretische Chemie, Physikalisch-Chemisches Institut, Universität Heidelberg, 69120 Heidelberg, Germany*
[3]*Institut Lumière Matière, UMR5306—UCBL and CNRS, 69622 Villeurbanne, France*

We report the experimental observation of quantum interference in the nuclear wave-packet dynamics driving ultrafast excitation-energy transfer in argon dimers below the threshold of interatomic Coulombic decay (ICD). Using time-resolved photoion-photoion coincidence spectroscopy and quantum dynamics simulations, we reveal that the electronic relaxation dynamics of the inner-valence $3s$ hole on one atom leading to a $4s$ or $4p$ excitation on the other one is influenced by nuclear quantum dynamics in the initial state, giving rise to a deep, periodic modulation on the kinetic-energy-release (KER) spectra of the coincident Ar^+-Ar^+ ion pairs. Moreover, the time-resolved KER spectra show characteristic fingerprints of quantum interference effects during the energy-transfer process. Our findings pave the way to elucidating quantum-interference effects in ultrafast charge- and energy-transfer dynamics in more complex systems, such as molecular clusters and solvated molecules.

Atoms and molecules can absorb photons of energy exceeding the binding energies of their core or inner-valence electrons, forming highly excited cationic states that can relax through fluorescence or Auger decay. An isolated atom or molecule with an inner-valence vacancy will in general not have enough excess energy to undergo Auger decay, and will relax by fluorescence or, in the case of molecules, also by a coupling to nuclear dynamics, both of which are relatively slow processes. In 1997, Cederbaum *et al.* [1] proposed a new mechanism of ultrafast electronic decay in which the environment plays a crucial role, termed intermolecular(atomic) Coulombic decay (ICD). In this mechanism an inner-valence hole can transfer its energy to a neighboring species which subsequently releases the excess energy by emitting an electron from its outer-valence shell. After both theoretical [2–9] and experimental [10–16] studies over more than two decades, ICD was found in a large variety of weakly bound systems, including liquid water [17]. ICD has been proven to be a very efficient process that typically dominates over other relaxation channels. Moreover, as a purely electronic energy-transfer mechanism that does not depend on the presence of particular resonances or on the coupling of electronic excitations to nuclear motion present in many molecular processes, ICD offers an efficient way to redistribute the locally deposited energy within weakly bound systems (for a recent review, see Ref. [18]).

Interestingly, for all homonuclear noble-gas dimers heavier than neon, the ICD channel of the inner-valence hole state is energetically closed. For example, in Ar atoms the $3s$ ionization energy is 29.24 eV which is below the threshold for ICD at 31.52 eV [19]. However, a recent pioneering study on the argon dimer [20] revealed that although the relaxation energy of the $3s$ hole on one atom is not enough to ionize the neighboring atom, it is sufficient to excite an electron of the latter to Rydberg states, creating a dissociative Ar^+-Ar^* system. This process can be called pre-ICD or frustrated ICD [19,21].

Here, we report the discovery of quantum-interference effects in the nuclear dynamics that mediate the ultrafast interatomic energy-transfer process (or frustrated ICD) in argon dimers. We find that this quantum interference strongly modulates the energy-transfer probability as a function of time elapsed since the excitation process. As illustrated in Fig. 1(a), an extreme-ultraviolet (XUV) pulse (magenta) creates a $3s$ hole in one of the Ar atoms of the dimer, followed by the ultrafast transfer (green) of excitation energy to the neighboring argon. A delayed infrared (IR) pulse (red) can then ionize the excited electron from the neighboring atom, which initiates a Coulomb explosion (orange) of the two cations. By monitoring the kinetic-energy-release (KER) spectrum of coincident Ar^+-Ar^+ ions, one can directly reconstruct the nuclear dynamics in this ultrafast interatomic energy-transfer process. The equilibrium internuclear distance of the neutral argon dimer is 3.8 Å, corresponding to a KER of around 3.8 eV. Because the frustrated-ICD final state, Ar^+-$Ar^*(3p^{-1}nl)$, is a dissociative state, the corresponding KER signal is expected to appear at and below 3.8 eV. Note that the
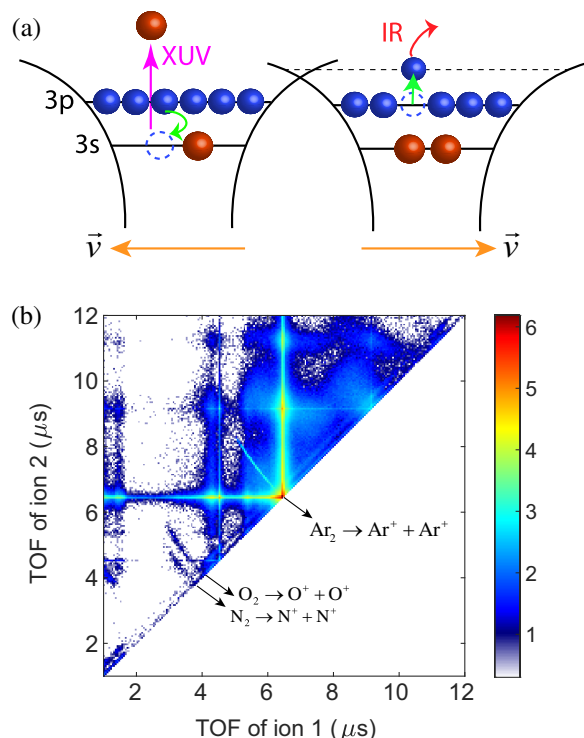
FIG. 1. (a) Illustration of the pump-probe principle for measuring the frustrated-ICD process of the $3s$ hole in an argon dimer. The XUV-pump pulse removes a $3s$ electron from one of the atoms of the dimer (magenta arrow) initiating a frustrated-ICD process, in which a $3p$ electron fills the $3s$ vacancy transferring the released energy to the other argon atom where an electron is excited to a $4s$ or $4p$ orbital (green arrows). The excited electron is then ionized by a delayed IR pulse (red arrow) creating a dication that undergoes a Coulomb explosion. (b) Measured photoion-photoion coincidence (PIPICO) spectrum, where the XUV-IR delay was integrated from zero to 2 ps.

frustrated ICD itself (i.e., in the XUV-only case) does not contribute to the Coulomb explosion signal, as opposed to the ICD process of satellite states $Ar^+(3p^{-2}nl)$-Ar created by shake-up ionization [22–24]. In an IR field, the satellite states can be ionized and then decay through the radiative charge transfer (RCT) process $Ar^{2+}(3p^{-2})$-Ar $\rightarrow$ Ar^+-Ar^+ [25,26] when the internuclear distance is shrinking, corresponding to a KER peak centered at 5.3 eV. In our experiments, we did not observe the shake-up ICD channel due to its low cross section in our energy regime.

Experimentally, the XUV pulses are obtained from high-order harmonic generation (HHG) by focusing a 30-fs IR pulse into a 3-mm-long gas cell filled with 40 mbar of krypton, with the discrete odd harmonics ranging from 17 eV to 38 eV after spectral filtering through a 200-nm-thick aluminum foil. The XUV-IR cross-correlation signal is measured to be around 40 fs. The time zero is accurately calibrated by the delay-dependent Ar^{2+} yield (not shown) from monomers due to the laser-enabled Auger decay [27]. The intensity of the IR pulse is controlled at around

6×10^{12} W/cm^2, which is too weak to ionize neutral argon atoms on its own. The XUV and IR pulses are both focused into the reaction center of the cold target recoil ion momentum spectroscopy (COLTRIMS) reaction microscope [28,29], where the supersonic gas jet of argon atoms (backing pressure of 1 bar) is delivered by a small nozzle with an opening-hole diameter of 30 μm and passed through two conical skimmers located 10 mm and 30 mm downstream with a diameter of 0.2 mm and 1 mm, respectively. The fraction of dimers relative to monomers is measured to be about 3%. In the COLTRIMS spectrometer, a relatively strong static electric field ($\sim$7.7785 V/cm) is applied to collect the ions with high kinetic energies and thus the electron detector is not used.

The measured delay-averaged photoion-photoion coincidence (PIPICO) spectrum is reported in Fig. 1(b), where the diagonal-like features correspond to the ion pairs in Coulomb explosion channels. The signal converging to the time-of-flight (TOF) of 6.4 μs is the reaction pathway $Ar_2 \xrightarrow{XUV+IR} Ar^+$-$Ar^+$, which we are interested in. Using a three-dimensional recoil momentum sphere as a confinement condition in off-line data analysis, we can only pick up the events in this channel and rule out the contribution from residual N_2 and O_2 gases in the reaction chamber.

The measured time-resolved KER spectra of the coincident Ar^+-Ar^+ channel are shown in Fig. 2(a). Comparing with the previous study [20], our result validates that there are two clearly visible decay channels approaching 0.8 eV
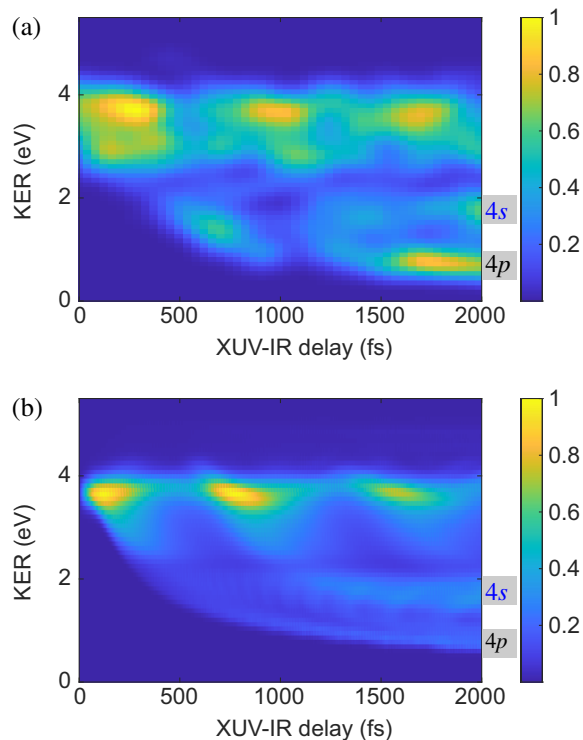

FIG. 2. Measured (a) and calculated (b) time-resolved KER spectra of the Coulomb explosion channel of Ar_2.

and 1.9 eV at the largest pump-probe delays, which are identified as $4p$ and $4s$ excited states in the neighboring atoms, respectively. What we observed exclusively in this work is the periodic modulation on the main island at 3.8 eV. The oscillation period is about 800 fs, a typical timescale of vibrational motions of noble-gas dimers. This is reminiscent of the nuclear dynamics in this ultrafast interatomic energy-transfer process.

To interpret our experimental results, we performed quantum dynamics simulations of the process and computed the time-dependent KER spectra in the framework of nuclear wave packets propagating on the potential-energy curves (PECs) of the involved states. The *ab initio* PECs of the ground and the final $Ar^+(3p^{-1})$-$Ar^+(3p^{-1})$ states are taken from Ref. [22], while the PECs of the initial and final states for the frustrated-ICD process, namely, $Ar^+(3s^{-1})$-Ar, and $Ar^+(3p^{-1})$-$Ar^*(3p^{-1}4s)$ and $Ar^+(3p^{-1})$-$Ar^*(3p^{-1}4p)$, are taken from Ref. [20] and depicted in Figs. 3(a) and 3(b). The complete set of PECs can be found in Ref. [30]. Despite the high-level electronic-structure method used to compute the $3s^{-1}$ PECs (the non-Dyson-ADC(3) Green's function approach [31]), the potential-energy wells appear to be slightly deeper, resulting in a shorter oscillation period compared to the experimentally observed one. To correct for this, the ungerade *ab initio* $3s^{-1}$ PEC was first fitted to a Morse potential and then its parameters optimized such that the wave-packet motion reproduces the experimentally observed period of about 800 fs. The Morse-potential parameters were ($D_e = 0.129$ eV, $R_e = 3.03$ Å, $\alpha = 0.91$ 1/a.u.) from the *ab initio* calculations and ($D_e = 0.064$ eV, $R_e = 3.03$ Å, $\alpha = 0.78$ 1/a.u.) after optimization. Such an adjustment of PECs of rare-gas dimers has already been successfully used in the past (see, Ref. [32]).

To simulate the energy transfer from $Ar^+(3s^{-1})$-Ar to $Ar^+(3p^{-1})$-$Ar^*(3p^{-1}4s)$ and $Ar^+(3p^{-1})$-$Ar^*(3p^{-1}4p)$, taking place at the points of curve crossings, we introduced an effective decay width, which corresponds to the energy-transfer time of $\tau_{3s} = 824 \pm 183$ fs extracted in Ref. [20]. The corresponding decay width of 0.8 meV was statistically distributed to the respective $4s$- and $4p$-excited states according to their multiplicity. The effective decay widths are then associated with each state and introduced with step functions at the corresponding curve crossings. This approach allows us to use the same coupled set of time-dependent Schrödinger equations to describe the nuclear dynamics as for ICD (see, e.g., Refs. [4,7,33]).

The simulation assumes a broad-band ionization with the XUV-pump pulse, promoting the vibrational ground state of Ar_2 to the $Ar^+(3s^{-1})$-Ar PEC. This initial wave packet is then propagated with a Hamiltonian containing all the states involved in the frustrated-ICD process [see Figs. 3(a) and 3(b)] coupled with the respective decay widths. This approach follows the well-established method to treat electronic decay processes accounting for the nuclear
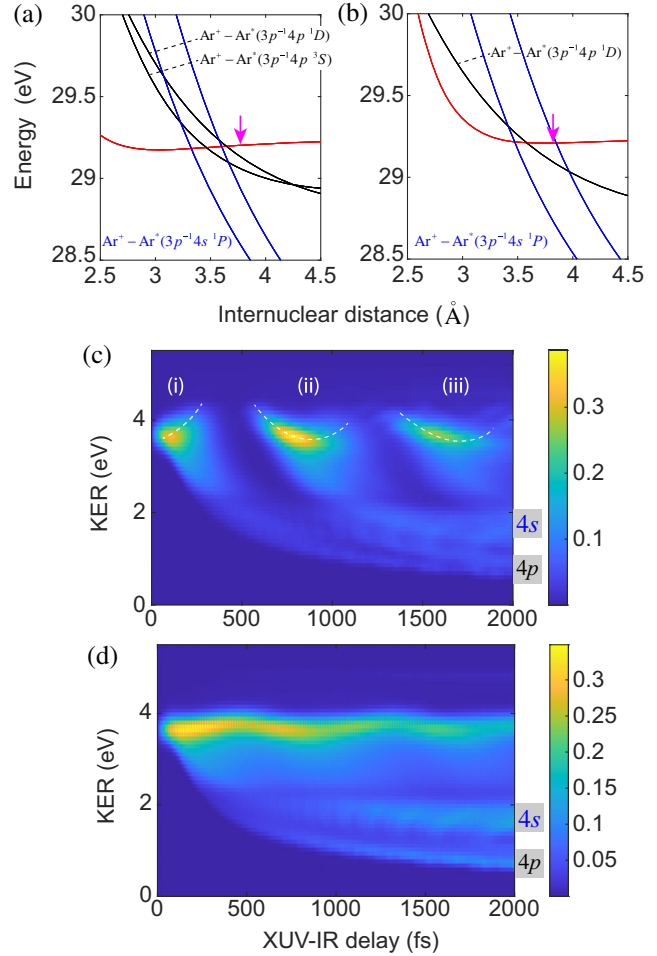

FIG. 3. Potential-energy curves of argon dimers relevant for the process belonging to ungerade $^2\Sigma_u^+$ (a) and gerade $^2\Sigma_g^+$ (b) symmetry, taken from Ref. [20]. The magenta arrows indicate the equilibrium internuclear distance of the ground state of the neutral dimer, i.e., the center of the Franck-Condon region. (c),(d) Calculated time-resolved KER spectra from the ungerade and gerade states, respectively.

dynamics of the system introduced in Refs. [34,35]. The wave-packet propagation is performed with the complex short iterative Lanczos integrator [36] implemented in the Heidelberg MCTDH package [37]. To get the KER spectrum at each time step ($\Delta\tau = 5$ fs), the wave packet propagating on the $4s$- or $4p$-excited state is promoted to the final repulsive dicationic state, simulating the ionization by the IR-probe pulse. This procedure is separately repeated for each gerade and ungerade transition between the $3s$-hole and $4s$- or $4p$-excited state. Finally, the gerade and ungerade contributions are incoherently summed up in order to construct the time-resolved XUV-IR KER spectra shown in Fig. 2(b).

As we see from Fig. 2, the computed time-dependent KER spectra is in good agreement with the experimental one. The structures converging to 0.8 eV and 1.9 eV, associated with the probing of the $4p$- and $4s$-excited state,

respectively, the three intense islands at 3.8 eV, resulting from the oscillation of the wave packet in the $3s^{-1}$ potential well, and the lack of signal at 2.3 eV, due, as we will see, to a destructive interference, are well reproduced. This allows us to analyze in detail the quantum dynamics along the frustrated-ICD process and the various features observed in the measured KER spectra. We note that the $4p$ channel is observed to dominate over the $4s$ channel, which is not reproduced by our quantum simulations. This can be attributed to the different probe efficiencies, due to the different energy gaps between the dissociating $4p/4s$ states and the final Coulomb repulsive state requiring different numbers of probe-pulse photons. This effect is not taken into account in our simulations, which assume equal ionization cross sections for the two channels.

Let us start with the slightly parabolic shapes of the three main islands at 3.8 eV. This reflects the motion of the wave packet on the $3s$-hole state and the fact that the curve crossings with the $4s$- and $4p$-excited states are reached one after the other. The wave packet on the $3s$-hole potential is initially localized around the equilibrium internuclear distance of the neutral dimer [marked by magenta arrows in Figs. 3(a) and 3(b)], and then starts to propagate towards the potential minimum passing through all the curve crossings, where the population transfers to the $4s$- and $4p$-potentials take place. Because decreasing internuclear distances appear as increasing KER in the spectra, the first island (between 0 and 500 fs) has an increasing parabolic shape. After the wave packet passes the last curve crossing and moves until its left turning point and back in the $3s^{-1}$ potential well, no frustrated ICD takes place and correspondingly the KER signal disappears. On its way back, while moving towards increasing internuclear distances, the wave packet passes the curve crossings in a reversed order, making the KER signal appear as a decreasing parabola up to about 800 fs when the first oscillation is completed and the process starts again. This motion of the wave packet and the decay at the respective curve crossings is schematically depicted in Figs. 4(i) and 4(ii). During its motion, the wave packet expands and develops structure [Fig. 4(iii)] making the signal fade out and blur with increasing pump-probe delay time.

By separating the gerade and ungerade contributions of the spectra, we can get additional insights into nuclear dynamics. Those are shown in Fig. 3(c) for the ungerade states, and in Fig. 3(d) for the gerade states. The most significant difference between the two is the signal around 3.8 eV, appearing as clear islands in the ungerade case and as a wavelike structure in the gerade spectra. The reason lies in the shape of the $3s^{-1}$ potential and the positions of the curve crossings. The gerade-symmetry PEC is shallower and the curve crossings are closer to the potential minimum and the inner turning point [compare Figs. 3(a) and 3(b)]. Consequently, the oscillation period for the
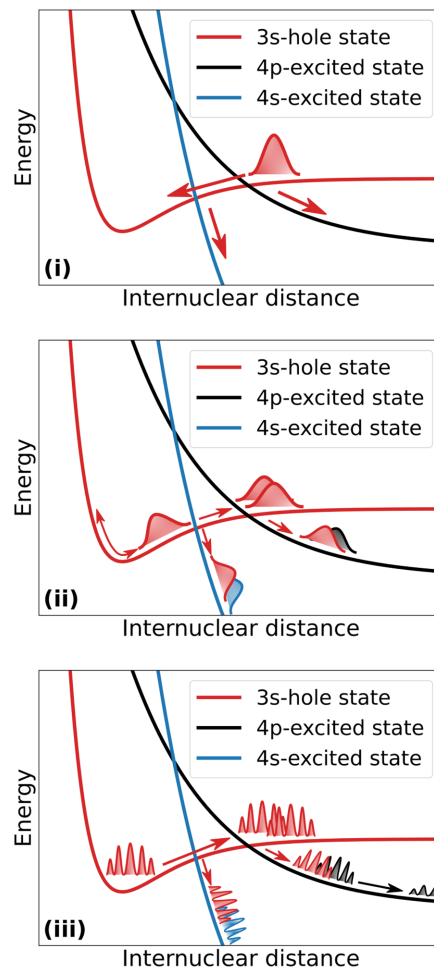

FIG. 4. (i)–(iii) Schematic representation of nuclear dynamics in Ar$_2$ during frustrated ICD in the XUV-IR-delay ranges (i), (ii), and (iii), as defined in Fig. 3. The red, blue, and black curves represent the $3s$-hole [Ar$^{+*}(3s^{-1})$-Ar], $4s$-, and $4p$-excited [Ar$^{+}(3p^{-1})$-Ar$^{*}(3p^{-1} 4s/4p)$] states, respectively. The arrows mark the propagation direction.

gerade contribution is slightly longer and as some portion of the wave packet is always at the curve crossings, the signal at 3.8 eV does not disappear. The wavelike shape, however, clearly reflects the back-and-forth motion of the wave packet.

We now return to the lack of signal around 2.3 eV, appearing in both gerade and ungereade spectra, and clearly visible also in the experimental KER trace [see Fig. 2(a)]. Our analysis shows that this is a result of a destructive interference taking place between different portions of the wave packet transferred to the $4s$- and $4p$-excited potentials at two consecutive passages through the corresponding curve crossings. In other words, during its excursion to the inner turning point and back, the wave packet moving on the $3s^{-1}$ PEC accumulates a phase that is close to an odd multiple of π and when transferred to $4s$ and $4p$ potentials interferes destructively with the portions of the wave

packet already propagating on these PECs [see Figs. 4(ii) and 4(iii)].

Before we conclude, we would like to briefly comment on one feature in the measured KER spectra that is not reproduced by the simulations. This is the decrease in the signal between 800 fs and 1200 fs of the trace converging to 0.8 eV and reflecting the dynamics on the PEC of the $4p$-excited state. A possible explanation of this feature could be that around 1 ps after the energy transfer, the wave packet propagating on the $4s$ state can be efficiently transferred to a higher excited $Ar^+(3p^{-1})$-$Ar^*(3p^{-1}nl)$ state by a single IR photon, thus removing the population from the measured Ar^+-Ar^+ signal. Indeed, the ionization of the $4p$ electron needs between 2 and 3 photons, depending on the internuclear distance, and a resonance condition with a single photon will easily hinder the multiphoton ionization channel. A possible candidate is the $Ar^+(3p^{-1})$-$Ar^*(3p^{-1}4d)$ state which would satisfy the resonance condition, but the spectrum of excited states in this energy range is already so dense that a definitive assignment of such transitions becomes challenging.

In summary, we have demonstrated that high-resolution time-resolved photoion-photoion spectroscopy performed with high-harmonic sources can give access to the quantum nuclear dynamics underlying excitation-energy transfer, i.e., frustrated ICD, in argon dimers. The different features in the time-resolved KER spectra can be analyzed with the help of quantum wave-packet propagation simulations, leading to a detailed reconstruction of the nuclear dynamics throughout the process. The vibrational motion of the system in the initially populated $3s^{-1}$ state, as well as the interference of different portions of the wave packet transferred to the final $4s$- and $4p$-excited states at different times, lead to characteristic patterns in the time-resolved KER spectrogram. The high level of detail that can be achieved when analyzing the frustrated-ICD process in rare-gas dimers suggests that this technique can be used to study such energy-transfer processes in more complex systems like weakly bound molecular dimers, as well as (micro-)solvated molecules. We hope that our study will stimulate further efforts in this direction.

M. H. and J. F. contributed equally to this work.

*alexander.kuleff@pci.uni-heidelberg.de
†hwoerner@ethz.ch

[1] L. S. Cederbaum, J. Zobeley, and F. Tarantelli, Giant Intermolecular Decay and Fragmentation of Clusters, Phys. Rev. Lett. **79**, 4778 (1997).

[2] R. Santra, J. Zobeley, L. S. Cederbaum, and N. Moiseyev, Interatomic Coulombic Decay in van der Waals Clusters and Impact of Nuclear Motion, Phys. Rev. Lett. **85**, 4490 (2000).

[3] R. Santra and L. S. Cederbaum, Non-Hermitian electronic theory and applications to clusters, Phys. Rep. **368**, 1 (2002).

[4] S. Scheit, V. Averbukh, H.-D. Meyer, N. Moiseyev, R. Santra, T. Sommerfeld, J. Zobeley, and L. S. Cederbaum, On the interatomic Coulombic decay in the Ne dimer, J. Chem. Phys. **121**, 8393 (2004).

[5] V. Averbukh, I. B. Müller, and L. S. Cederbaum, Mechanism of Interatomic Coulombic Decay in Clusters, Phys. Rev. Lett. **93**, 263002 (2004).

[6] A. I. Kuleff and L. S. Cederbaum, Tracing Ultrafast Interatomic Electronic Decay Processes in Real Time and Space, Phys. Rev. Lett. **98**, 083201 (2007).

[7] P. V. Demekhin, Y.-C. Chiang, S. D. Stoychev, P. Kolorenč, S. Scheit, A. I. Kuleff, F. Tarantelli, and L. S. Cederbaum, Interatomic Coulombic decay and its dynamics in NeAr following K-LL Auger transition in the Ne atom, J. Chem. Phys. **131**, 104303 (2009).

[8] K. Gokhberg, P. Kolorenč, A. I. Kuleff, and L. S. Cederbaum, Site-and energy-selective slow-electron production through intermolecular Coulombic decay, Nature (London) **505**, 661 (2014).

[9] V. Stumpf, K. Gokhberg, and L. S. Cederbaum, The role of metal ions in x-ray-induced photochemistry, Nat. Chem. **8**, 237 (2016).

[10] S. Marburger, O. Kugeler, U. Hergenhahn, and T. Möller, Experimental Evidence for Interatomic Coulombic Decay in Ne Clusters, Phys. Rev. Lett. **90**, 203401 (2003).

[11] T. Jahnke, A. Czasch, M. S. Schöffler, S. Schössler, A. Knapp, M. Käsz, J. Titze, C. Wimmer, K. Kreidi, R. E. Grisenti, A. Staudte, O. Jagutzki, U. Hergenhahn, H. Schmidt-Böcking, and R. Dörner, Experimental Observation of Interatomic Coulombic Decay in Neon Dimers, Phys. Rev. Lett. **93**, 163401 (2004).

[12] Y. Morishita, X.-J. Liu, N. Saito, T. Lischke, M. Kato, G. Prümper, M. Oura, H. Yamaoka, Y. Tamenori, I. H. Suzuki, and K. Ueda, Experimental Evidence of Interatomic Coulombic Decay from the Auger Final States in Argon Dimers, Phys. Rev. Lett. **96**, 243402 (2006).

[13] N. Sisourat, N. V. Kryzhevoi, P. Kolorenč, S. Scheit, T. Jahnke, and L. S. Cederbaum, Ultralong-range energy transfer by interatomic Coulombic decay in an extreme quantum system, Nat. Phys. **6**, 508 (2010).

[14] K. Sakai, S. Stoychev, T. Ouchi, I. Higuchi, M. Schäffler, T. Mazza, H. Fukuzawa, K. Nagaya, M. Yao, Y. Tamenori, A. I. Kuleff, N. Saito, and K. Ueda, Electron-Transfer-Mediated Decay and Interatomic Coulombic Decay from the Triply Ionized States in Argon Dimers, Phys. Rev. Lett. **106**, 033401 (2011).

[15] X. Ren, E. Wang, A. D. Skitnevskaya, A. B. Trofimov, K. Gokhberg, and A. Dorn, Experimental evidence for ultrafast

intermolecular relaxation processes in hydrated biomolecules, Nat. Phys. **14,** 1062 (2018).

[16] X. Ren, J. Zhou, E. Wang, T. Yang, Z. Xu, N. Sisourat, T. Pfeifer, and A. Dorn, Ultrafast energy transfer between π-stacked aromatic rings upon inner-valence ionization, Nat. Chem. **14,** 232 (2022).

[17] P. Zhang, C. Perry, T. T. Luu, D. Matselyukh, and H. J. Wörner, Intermolecular Coulombic Decay in Liquid Water, Phys. Rev. Lett. **128,** 133001 (2022).

[18] T. Jahnke, U. Hergenhahn, B. Winter, R. Dörner, U. Frühling, P. V. Demekhin, K. Gokhberg, L. S. Cederbaum, A. Ehresmann, A. Knie, and A. Dreuw, Interatomic and intermolecular Coulombic decay, Chem. Rev. **120,** 11295 (2020).

[19] P. Lablanquie, T. Aoto, Y. Hikosaka, Y. Morioka, F. Penent, and K. Ito, Appearance of interatomic Coulombic decay in Ar, Kr, and Xe homonuclear dimers, J. Chem. Phys. **127,** 154323 (2007).

[20] T. Mizuno, P. Cörlin, T. Miteva, K. Gokhberg, A. Kuleff, L. S. Cederbaum, T. Pfeifer, A. Fischer, and R. Moshammer, Time-resolved observation of interatomic excitation-energy transfer in argon dimers, J. Chem. Phys. **146,** 104305 (2017).

[21] R. Thissen, P. Lablanquie, R. Hall, M. Ukai, and K. Ito, Photoionization of argon, krypton and xenon clusters in the inner valence shell region, Eur. Phys. J. D **4,** 335 (1998).

[22] T. Miteva, Y.-C. Chiang, P. Kolorenč, A. Kuleff, K. Gokhberg, and L. Cederbaum, Interatomic Coulombic decay following resonant core excitation of Ar in argon dimer, J. Chem. Phys. **141,** 064307 (2014).

[23] X. Ren, E. Jabbour Al Maalouf, A. Dorn, and S. Denifl, Direct evidence of two interatomic relaxation mechanisms in argon dimers ionized by electron impact, Nat. Commun. **7,** 1 (2016).

[24] J. Rist, T. Miteva, B. Gaire, H. Sann, F. Trinter, M. Keiling, N. Gehrken, A. Moradmand, B. Berry, M. Zohrabi *et al.*, A comprehensive study of interatomic Coulombic decay in argon dimers: Extracting R-dependent absolute decay rates from the experiment, Chem. Phys. **482,** 185 (2017).

[25] N. Saito, Y. Morishita, I. Suzuki, S. Stoychev, A. Kuleff, L. Cederbaum, X.-J. Liu, H. Fukuzawa, G. Prümper, and K. Ueda, Evidence of radiative charge transfer in argon dimers, Chem. Phys. Lett. **441,** 16 (2007).

[26] R. Johnsen and M. A. Biondi, Measurements of radiative charge-transfer reactions of doubly and singly charged rare-gas ions with rare-gas atoms at thermal energies, Phys. Rev. A **18,** 996 (1978).

[27] P. Ranitovic, X. M. Tong, C. W. Hogle, X. Zhou, Y. Liu, N. Toshima, M. M. Murnane, and H. C. Kapteyn, Laser-Enabled Auger Decay in Rare-Gas Atoms, Phys. Rev. Lett. **106,** 053002 (2011).

[28] R. Dörner, V. Mergel, O. Jagutzki, L. Spielberger, J. Ullrich, R. Moshammer, and H. Schmidt-Böcking, Cold target recoil ion momentum spectroscopy: A 'momentum microscope' to view atomic collision dynamics, Phys. Rep. **330,** 95 (2000).

[29] J. Ullrich, R. Moshammer, A. Dorn, R. Dörner, L. Schmidt, and H. Schmidt-Böcking, Recoil-ion and electron momentum spectroscopy: Reaction-microscopes, Rep. Prog. Phys. **66,** 1463 (2003).

[30] https://github.com/cxlsmiles/pecs_database.

[31] J. Schirmer, A. Trofimov, and G. Stelter, A non-Dyson third-order approximation scheme for the electron propagator, J. Chem. Phys. **109,** 4734 (1998).

[32] J. Fedyk, K. Gokhberg, T. Miteva, L. S. Cederbaum, and A. I. Kuleff, Interference effects in the photoelectron spectrum of the NeKr dimer and vibrationally selected interatomic Coulombic decay, Phys. Rev. A **107,** 023109 (2023).

[33] P. V. Demekhin, K. Gokhberg, G. Jabbari, S. Kopelke, A. I. Kuleff, and L. S. Cederbaum, Overcoming blockade in producing doubly excited dimers by a single intense pulse and their decay, J. Phys. B **46,** 021001 (2013).

[34] L. S. Cederbaum and F. Tarantelli, Nuclear dynamics of decaying states: A time-dependent formulation, J. Chem. Phys. **98,** 9691 (1993).

[35] E. Pahl, H.-D. Meyer, and L. S. Cederbaum, Competition between excitation and electronic decay of short-lived molecular states, Z. Phys. D **38,** 215 (1996).

[36] R. A. Friesner, L. S. Tuckerman, B. C. Dornblaser, and T. V. Russo, A method for exponential propagation of large systems of stiff nonlinear differential equations, J. Sci. Comput. **4,** 327 (1989).

[37] M. Beck, A. Jäckle, G. Worth, and H.-D. Meyer, The multiconfiguration time-dependent Hartree (MCTDH) method: A highly efficient algorithm for propagating wavepackets, Phys. Rep. **324,** 1 (2000).